

#### **Article**

Cite this article: Luo Y, Yin Y, Zhong Y, Lu X, Yang J, Sapkota L, Lu X, Liu Q (2025)
Dynamics of lake-terminating glaciers in the Himalaya and Southeastern Tibet between 1990 and 2020. *Journal of Glaciology* **71**, e113, 1–11. https://doi.org/10.1017/jog.2025.10088

Received: 9 January 2025 Revised: 25 August 2025 Accepted: 26 August 2025

#### **Kevwords:**

glacier change; Himalaya; lake-terminating glacier; proglacial lake; Southeastern Tibet

**Corresponding author:** Qiao Liu; Email: liuqiao@imde.ac.cn

Dynamics of lake-terminating glaciers in the Himalaya and Southeastern Tibet between 1990 and 2020

Yunyi Luo<sup>1,2</sup> , Yongsheng Yin<sup>1,2</sup>, Yan Zhong<sup>3</sup>, Xueyuan Lu<sup>1,2</sup>, Jiawei Yang<sup>1,2</sup> , Liladhar Sapkota<sup>1,2</sup>, Xuyang Lu<sup>1</sup> and Qiao Liu<sup>1</sup>

<sup>1</sup>Institute of Mountain Hazards and Environment, Chinese Academy of Sciences, Chengdu, China; <sup>2</sup>College of Resources and Environment, University of Chinese Academy of Sciences, Beijing, China and <sup>3</sup>Climate Change Impacts and Risks in the Anthropocene (C-CIA), Institute for Environmental Sciences, University of Geneva, Geneva, Switzerland

#### **Abstract**

Lake-terminating glaciers retreat and thin faster than land-terminating glaciers, yet their long-term dynamics remain underexplored. Using multi source–remote sensing data combined with glacier velocity and elevation change datasets, we investigated their distribution and evolution in the Himalaya and Southeastern Tibet from 1990 to 2020. By 2020, 577 lake-terminating glaciers (2561.5  $\pm$  11.8 km²) had been identified, representing ~2% of all glaciers by number and ~10% by area. Of these, 246 glaciers maintained contact with proglacial lakes (Type 1 change), while 331 developed new lakes (Type 2 change). Additionally, 173 glaciers detached from lakes (Type 3 change). Variations in glacier–lake contact strongly modulate glacier dynamics. Type 1 change glaciers experienced the largest area loss (73.8  $\pm$  13.1 km²), whereas Type 2 change glaciers showed the greatest average retreat distance (1.06  $\pm$  0.05 km). Among Type 1 change glaciers (>5 km²) with significant velocity trends, 22% accelerated and 78% decelerated, while all Type 3 change glaciers with significant velocity trends consistently decelerated. These findings underscore the pivotal influence of proglacial lake evolution on glacier dynamics, advancing our understanding of glacier–lake interactions on the Tibetan Plateau and beyond.

# 1. Introduction

As the largest mid-latitude repository of glaciers, High Mountain Asia (HMA) has experienced accelerated ice mass loss under climate warming, with a mass change rate of -20.1 Gt a<sup>-1</sup> from 2000 and 2019 (Hugonnet and others, 2021). This melting has driven substantial meltwater runoff, promoting the formation and expansion of glacial lakes. Satellite-based inventories document an 11% increase in the number of glacial lake (n = 27205 to 30121) and 15% expansion in total area (1806.5  $\pm$  2.1 and 2080.1  $\pm$  2.3 km $^2$ ) across HMA between 1990 and 2018 (Wang and others, 2020). These proglacial water bodies now exert fundamental controls on glacier flow dynamics (Pronk and others, 2021) and regional mass loss patterns (Tsutaki and others, 2019).

Proglacial lakes form behind the terminal moraine dams, originating from the coalescence of supraglacial ponds or lakes near glacier termini (Quincey and others, 2007; Carrivick and Tweed, 2013). These lakes amplify glacier mass loss rates and modify ice flow dynamics through two synergistic mechanisms: (1) subaqueous melting caused by thermal undercutting (Truffer and Motyka, 2016) and the calving process (Benn and others, 2007a) amplify frontal retreat; and (2) basal lubrication from reduced effective pressure elevates ice flow (Sugiyama and others, 2011; Sutherland others, 2020). Observations confirm these impacts: in the Everest region, lake-terminating glaciers lost mass 32% faster than land-terminating types during 2000-2015 (King and others, 2017). Across HMA, the mass loss rates of laketerminating glaciers exceeded regional averages by 18-97% (Brun and others, 2019), with recent evidence suggesting substantial underestimation of subaqueous melting impacts (Zhang and others, 2023). Correspondingly, lake-terminating glaciers exhibit two- to threefold higher velocities than their land-terminating counterparts (Pronk and others, 2021). Despite extensive research highlighting the profound impacts of proglacial lakes on glaciers, lake-induced effects propagate only through the lowermost ~30% of glacier length, with significant behavioral changes in glaciers occurring during advanced stages of lake evolution (Scoffield and others, 2024). This glacier-lake coupling establishes a positive feedback loop: lake expansion accelerates retreat, which in turn facilitates further lake growth. The evolving glacier-lake contact, driven by progressive terminus retreat, is anticipated to amplify spatial heterogeneity in glacial response behaviors. Crucially, understanding glacier behavior under changing glacierlake interaction not only reveals the nonlinear characteristics of glacial responses to climate

© The Author(s), 2025. Published by Cambridge University Press on behalf of International Glaciological Society. This is an Open Access article, distributed under the terms of the Creative Commons Attribution licence (http://creativecommons.org/licenses/by/4.0), which permits unrestricted re-use, distribution and reproduction, provided the original article is properly cited.

cambridge.org/jog



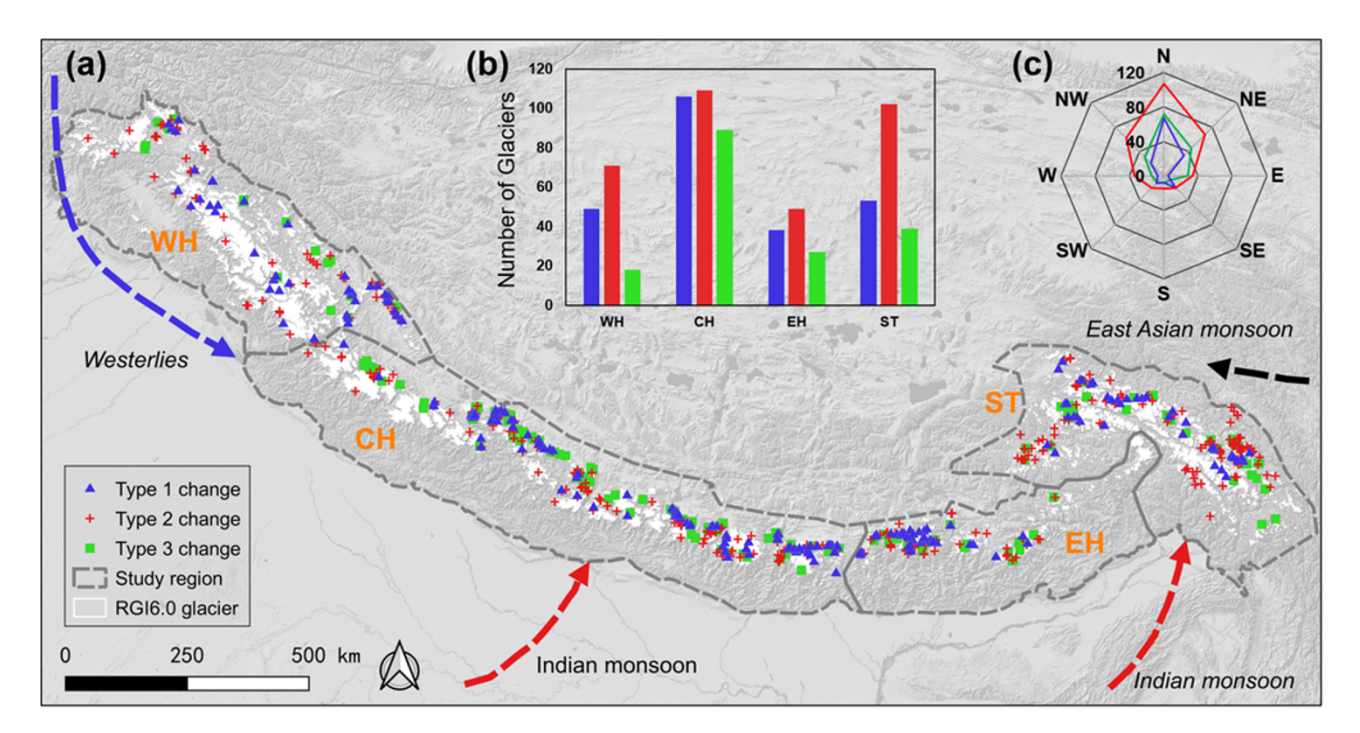


Figure 1. (a) Lake-terminating glacier distribution overview; (b) and (c) Numbers and aspect distributions of three different type of lake-terminating glaciers in four subregions. Type 1 change: Glaciers that remain in contact with proglacial lakes. Type 2 change: Glaciers with newly formed proglacial lakes. Type 3 change: Glaciers detached from proglacial lakes. WH: Western Himalaya. CH: Central Himalaya. EH: Eastern Himalaya. ST: Southeastern Tibet.

warming but also provides mechanistic support for water resource (Warren and Kirkbride, 2003) security assessments and disaster risk management.

The Himalaya and Southeastern Tibet host the highest concentration of lake-terminating glaciers within the HMA (Wang and others, 2020; Chen and others, 2021), with glaciers in these areas exhibiting the most negative mass balance in recent decades (Brun and others, 2017; Brun and others, 2019; Wang and others, 2020). With the continuing increase in both the number and size of proglacial lakes, investigating the distribution and changes of lake-terminating glaciers in the two regions is crucial for assessing and projecting glaciers' responses to climate change. Several studies have examined the spatiotemporal distribution of glaciers and glacial lakes in these regions. For example, Dou and others, (2023) who updated the glacier-lake inventory in Southeastern Tibet and analyzed its response to climate change, and Kumar and others, (2024) who monitored the spatiotemporal dynamics of glacial lakes in the Himachal Pradesh, Himalaya. However, systematic studies addressing the spatiotemporal distribution of the lake-terminating glacier-proglacial lake system and tracking changes in glacier-lake contact remain limited.

Therefore, this study focuses on lake-terminating glaciers with the following objectives: (1) to investigate their spatial distribution and spatiotemporal variability from 1990 to 2020 using multisource optical remote sensing datasets in the Himalaya and Southeastern Tibet; (2) to track the evolution of glacier-lake contact; and (3) to analyze the dynamics differentiation among lake-terminating glaciers.

# 2. The Himalaya and Southeastern Tibet regions

The Himalaya extends as an arcuate belt from Nanga Parvata in the west (about 8125 m a.s.l.) to Namcha Barwa in the east (about 7782 m a.s.l.). This cryospheric hotspot sustains 18874 glaciers, which are classified into temperate and continental cold glaciers. The region's climate system is governed by the Indian Ocean monsoon and secondary contributions from the westerlies. The region experiences wet seasons during both winter and summer, with the summer monsoon affecting the Eastern Himalaya and the winter monsoon primarily impacting the Western Himalaya (Bookhagen and Burbank, 2010). The extreme topography of the Himalaya blocks monsoonal air, resulting in relatively dry conditions on the northern slopes (Ageta and Higuchi, 1984).

The Southeastern Tibet (ST) encompasses the eastern regions of Nyainqentangla, Gangri Garpo, Goikarla Rigyu, and the western section of the Hengduan mountains. The region has an average elevation exceeding 3900 m a.s.l., with some areas rising above 7000 m a.s.l. Its climate system is governed by the Indian monsoon and the East Asian monsoon during the summer and spring, bringing abundant precipitation accompanied by warm conditions. The rainy season typically lasts from May to October each year. This region contains 7472 temperate glaciers, most of which are distributed above 3000 m a.s.l. and concentrated in the eastern Nyainqentanglha Mountains.

We divided the Himalaya and Southeastern Tibet into four subregions (Fig. 1a): Western Himalaya (WH), Central Himalaya (CH), and Eastern Himalaya (EH) and Southeastern Tibet (ST, including eastern of Nyainqentangla, Gangri Garpo, Goikarla Rigyu and western of Hengduan). In total, the study area contains 26346 glaciers with a combined area of 25900.5 km² (RGI6.0).

#### 3. Data and methods

# 3.1. Proglacial lakes inventory

The methodological framework for constructing a laketerminating glacier inventory requires accurate delineation

Table 1. Overview of the dataset used in this study

Dataset	Data type	Data period	Reference/link
RGI6.0 Glacier Inventory	Vector	1950-2010	RGI Consortium, 2017
SRTM DEM	Raster (30 m)	2000	https://www. earthdata.nasa. gov/
ITS_LIVE Glacier Velocity	Raster (120/240 m)	1985–2018	Dehecq, 2018
Glacier Elevation Change	Raster (100 m)	2000–2020	Hugonnet, 2021
OGGM Glacier Flowlines	Vector		Maussion, 2019
Landsat TM/OLI	Raster (30 m)	~1972	https:// earthexplorer.usgs. gov/
PlanetLabs	Raster (3 m)	~2014	https://www.planet.

of proglacial lakes as a prerequisite step. Proglacial lakes were automatically mapped using a workflow implemented in Google Earth Engine (GEE).

Landsat (TM/ OLI) imagery (Table 1) was employed to map proglacial lakes due to its five-decade temporal coverage (1972-present), suitable spatial resolution (30 m), global availability and open-access policy. The Landsat products provided by GEE were preprocessed, including radiometric calibration, atmospheric correction and geometric correction. To minimize the influence of ice and seasonal snow cover, as well as annual changes of lake-terminating glaciers and proglacial lakes, we selected images acquired during summer and autumn (July to November). Twotime windows, 1990  $\pm$  2 and 2020  $\pm$  1, were chosen to reveal the present and past state of glacial lakes. This study focuses on identifying glacier-contact lakes, therefore the investigation was limited to a 2 km buffer zone around glaciers. In total, 841 Landsat Thematic Mapper (TM) scenes were used for the 1990 period (Figures S1 and S2) and 1133 Landsat Operational Land Imager (OLI) scenes for the 2020 period (Figures S3 and S4). To reduce the effect of cloud coverage, we applied the C Function of Mask (CFMask) algorithm (Foga and others, 2017) to detect and remove the cloud before mosaicking the imagery.

An automated mapping algorithm based on hierarchical image segmentation and terrain analysis was employed to delineate glacial lake extents (Li and Sheng, 2012; Zhang and others, 2017). The Normalized Difference Water Index (NDWI; [(GREEN -NIR)/(GREEN + NIR)]) was employed to extract proglacial lakes. To reduce disturbances from mountain shadows, a slope threshold of <20° and a shaded relief threshold of >0.25 were applied (Zheng and others, 2021). An example is given in Figure S5. Previous studies exhibit variability in minimum area threshold for glacial lake identification. For example, Wang and others, (2020) set the threshold to 0.0054 km<sup>2</sup>, Chen and others, (2021) set it to 0.0081 km<sup>2</sup>, Luo and others, (2020) set it to 0.0036 km<sup>2</sup> and Li and others, (2020) set it to 0.01 km<sup>2</sup>. Smaller lake areas generally lead to greater error identification (Salerno and others, 2012). To identify lake-terminating glaciers as accurately as possible, this study adopts a minimum lake area threshold of 0.0036 km<sup>2</sup> (at least four pixels), following Luo and others, (2020). Proglacial lake datasets were cross-referenced with RGI6.0 glacier inventory to identify lake-terminating glaciers. Finally, careful visual inspection and manual re-editing were performed to correct misclassified glacial lakes and identify lake-terminating glaciers, using Landsat images, Planet Labs (Table 1), online maps (Google

Earth, Esri basemap, etc.) and other glacial lake datasets (Wang and others, 2020; Chen and others, 2021; Zheng and others, 2021).

The uncertainty ( $\lambda$ ) and relative error ( $E_g$ ) in glacier area was estimated to using the equation (Bolch and others, 2010):

$$\lambda = N \times \frac{G^2}{2} \tag{1}$$

$$E_{\rm g} = \frac{\lambda}{\rm S} \times 100\% \tag{2}$$

where N is the total count of pixels along the outline of ice coverage, G is the spatial resolution of the images used and S is the glacier area. The uncertainty  $(\delta)$  and relative error  $(E_l)$  of glacial lake area was estimated using the equation (Hanshaw and Bookhagen, 2014):

$$\delta = \frac{P}{G} \times \frac{G^2}{2} \times 0.6872 \tag{3}$$

$$E_l = \frac{\delta}{A} \times 100\% \tag{4}$$

where P is the perimeter of the glacial lake and A is the glacial lake area.

Then the accumulation of the study region can be calculated using the following equation based on error propagation theory (Wang and others, 2020):

$$E_T = \sqrt{\sum_{i=1}^n a_i^2} \tag{5}$$

where  $E_T$  is the area error of the entire study region or subregions, i is the glacier or lake of no. i in the entire study region or subregion and a is the error area. The error for calculation of changes in glacier and glacial lake area (ds) is obtained by:

$$ds = \sqrt{{S_1}^2 + {S_2}^2} \tag{6}$$

where  $S_1$  and  $S_2$  are the glacier or glacial lake areas at the beginning and end of the period.

# 3.2. Lake-terminating glacier identification and classification

In this study, lake-terminating glaciers are defined as glacier forming proglacial lakes along the direction of ice flow. Their classification was based on the glacier-lake contact change from 1990 to 2020. The identification of glacier-lake contact followed a twostage procedure: (1) Preliminary screening was conducted using spatial intersection analysis between glacier boundaries and icemarginal lakes, with a 500 m buffer tolerance. (2) Manual verification employed period-specific criteria. For the 2020 assessments, multi-source moderate- to high-resolution imagery (Planet Labs, Landsat, Google Earth, Esri basemaps, etc.) was used. Glacier-lake contact was confirmed when proglacial lakes overlapped with glacier terminus and exhibited diagnostic features such as terminal ice cliffs or transverse crevasses perpendicular to the flow direction. Evaluations for 1990 faced inherent uncertainties due to the limited spatial resolution of Landsat products (30 m), particularly for smaller glaciers where boundary delineation errors increased with decreasing glacier size. To address this, temporal cross-validation was applied: glaciers with ambiguous glacier-lake contacts were classified as interactive if sequential imagery from

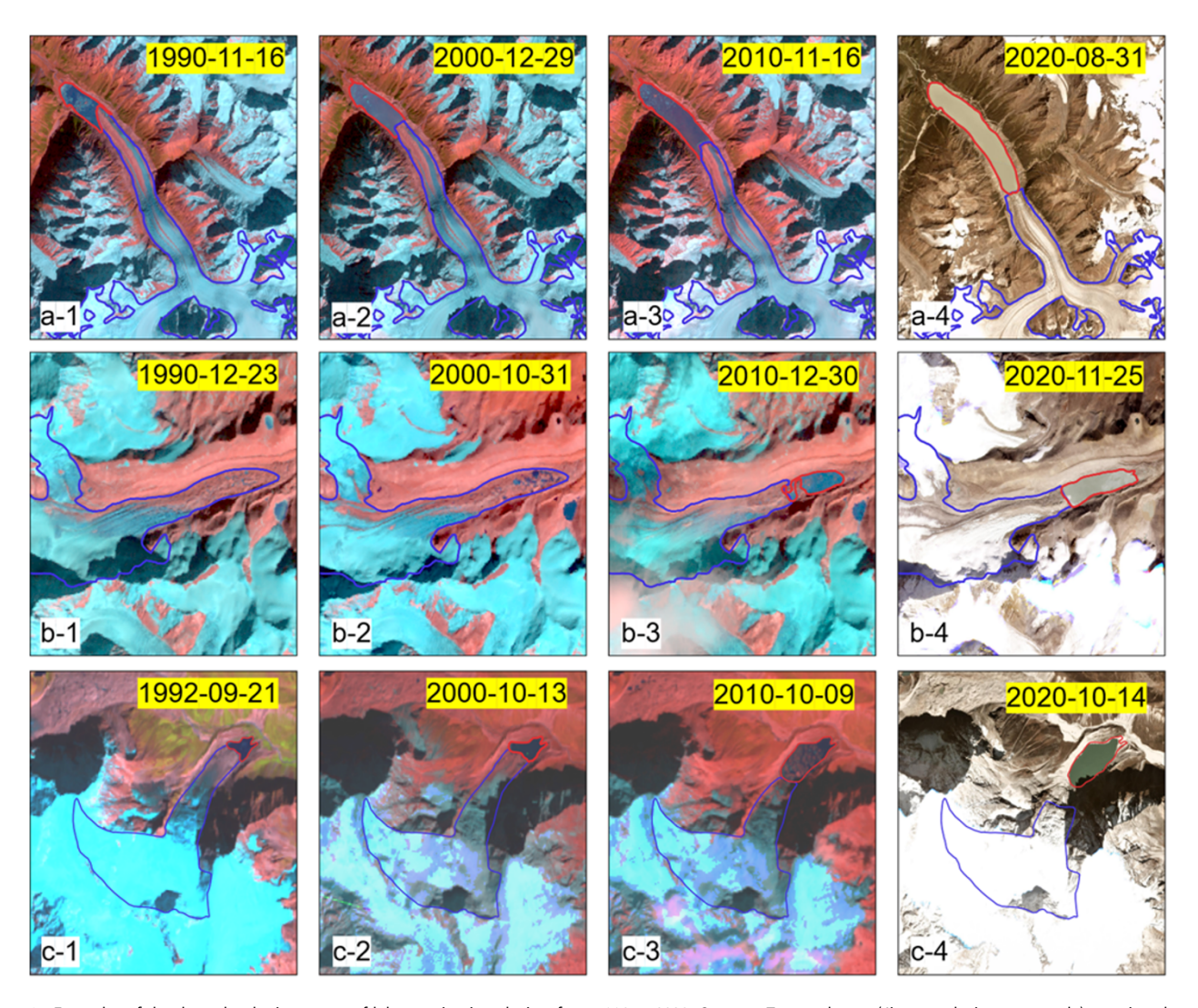


Figure 2. Examples of the three developing stages of lake-terminating glaciers from 1990 to 2020. Group a: Type 1 change (Jiongpu glacier as example), terminus keeping connected with proglacial lake. Group b: Type 2 change (Unnamed Glacier, RGI id: RGI60-15.03150, as example), terminus experienced transition from supraglacial lake to proglacial lake. Group c: Type 3 change (Jialong Co glacier as example), terminus experienced detach from proglacial lake.

1990 to 2020 showed lake expansion toward glacier termini. Lake-terminating glaciers were further categorized into three types: persistent glacier–lake connectivity (Type 1 change, Fig. 2a), transition from supraglacial lake to proglacial lake (Type 2 change, Fig. 2b) and detachment of proglacial lakes from parent glaciers (Type 3 change, Fig. 2c).

# 3.3. Analysis of glacier changes

Glacier surface elevation change data from Hugonnet and others, (2021) (Table 1) were extracted for glaciers larger than  $2 \,\mathrm{km^2}$ . Data points were excluded if the 19-year elevation change exceeded five times the normalized median absolute deviation within each elevation bin (Agarwal and others, 2023), following the methodology of Hugonnet and others, (2021). Glacier velocity data were obtained from ITS\_LIVE (Table 1) for glaciers exceeding  $2 \,\mathrm{km^2}$ . Pixels with velocity errors greater than  $5 \,\mathrm{m\,a^{-1}}$  were removed in accordance with the method of Dehecq and others, (2018).

To facilitate the delineation of glacier ablation zones and the interpretation of surface velocity patterns, we followed the approach of Hugonnet and others, (2021) and used the SRTM DEM to divide each glacier into 10 standardized elevation bins. These bins were then indexed from 0.1 to 1.0 according to their relative distance from the glacier terminus.

Due to higher measurement uncertainties in accumulation zones caused by low image contrast, the analysis of velocity anomaly was confined to the lower half of each glacier (0.1–0.5 elevation bins), which approximates the ablation zone (Dehecq and others, 2018). Velocity anomaly was calculated as the difference between the annual glacier velocity and the multi-year mean velocity.

Center flowlines were generated using the Open Global Glacier Model (OGGM) (Maussion and others, 2019) with a slightly adapted algorithm from (Kienholz and others, 2014), and manually adjusted using Landsat-5/8 satellite imagery and ice flow velocity data from ITS\_LIVE to ensure center flowlines terminated at the glacier termini in 1990 and 2020 and followed the main flow tributaries. Two sets of center flowline data, corresponding to the glacier terminus positions in 1990 and 2020, were then used to calculate the retreat of lake-terminating glaciers over this period.

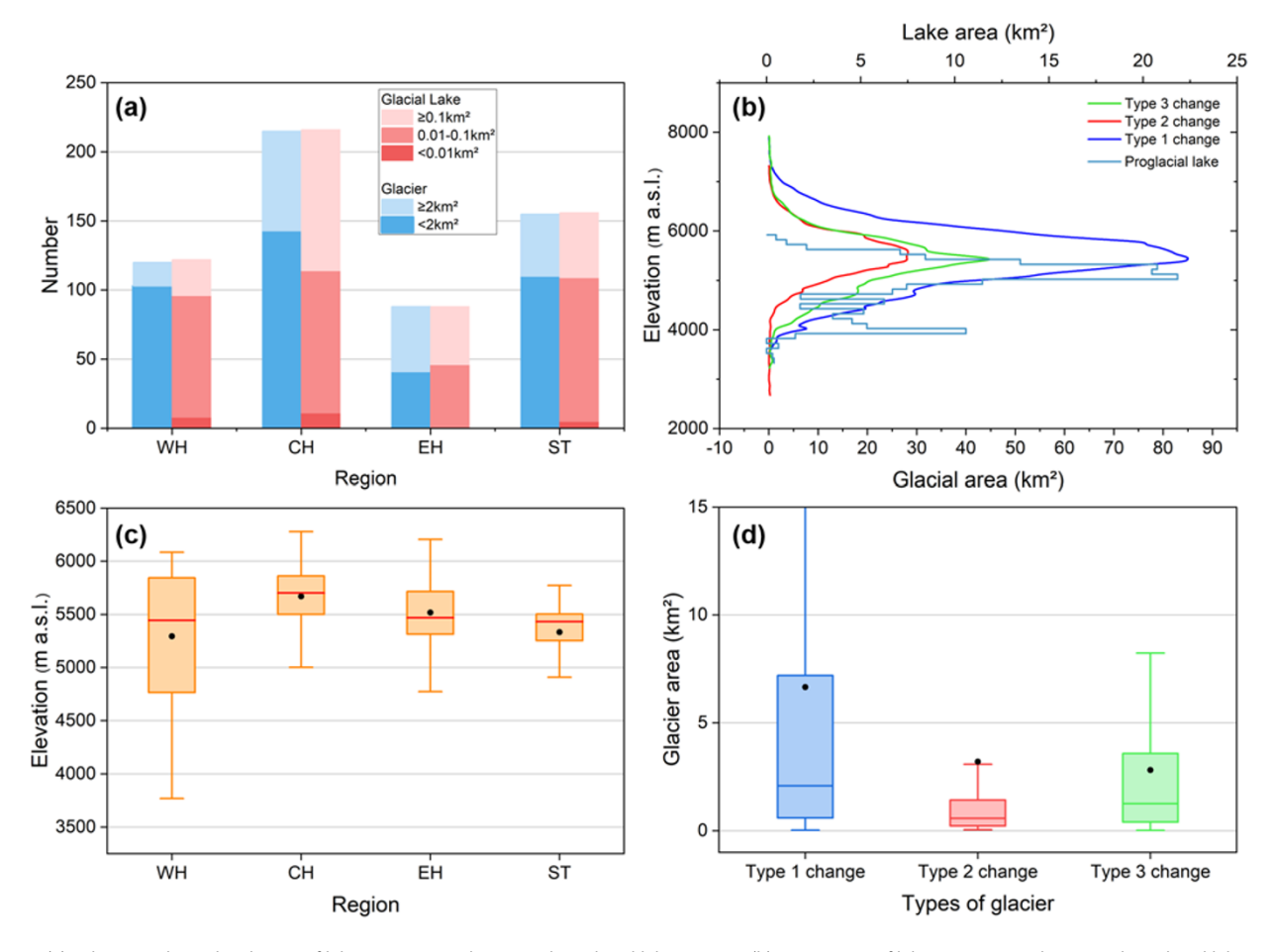


Figure 3. (a) Sub-regional size distribution of lake-terminating glaciers and proglacial lakes in 2020. (b) Hypsometry of lake-terminating glaciers and proglacial lakes in 2020. (c) Elevation distribution of lake-terminating glaciers in four subregions in 2020. (d) The area distribution of different types of glaciers in 2020. Type 1 change: Glaciers that remain in contact with proglacial lakes. Type 2 change: Glaciers with newly formed proglacial lakes. Type 3 change: Glaciers detached from proglacial lakes. In figures (c) and (d), the boxplots represent the interquartile range (IQR), the bars indicate the median and the dots represent the mean. WH: Western Himalaya. CH: Central Himalaya. EH: Eastern Himalaya. ST: Southeastern Tibet.

#### 4. Results

# 4.1. Distribution of lake-terminating glaciers

Our 2020 inventory identified 577 lake-terminating glaciers, representing approximately 2% of the glaciers in the RGI 6.0 database, with a cumulative area of 2561.5 ± 11.8 km<sup>2</sup>. Among these, 396 glaciers (~69%) had areas below 2 km<sup>2</sup> (Fig. 3a). The Central Himalaya hosted the highest number of lake-terminating glaciers, totaling 215 (~37%, Fig. 1b), whereas Southeastern Tibet exhibited the largest mean glacier size (6.7 km<sup>2</sup>), excluding the Yanong Glacier in Gangri Garpo, which covers approximately  $179.2 \pm 2.1 \text{ km}^2$  with a length of ~19.35 km. From 1990 to 2020, the total glacier area decreased by  $\sim 1.5 \pm 3.0 \text{ km}^2$ , and the glacier terminus retreated by about 0.31 km (Fig. 3a). Lake-terminating glaciers are predominantly located at altitudes of 5000 to 6000 m a.s.l. (Fig. 3b). Regionally, those in the Central Himalaya exhibit the highest average elevation (5669 m a.s.l), in contrast to the Western Himalaya, which shows the lowest mean elevation (5295 m a.s.l, Fig. 3c). Most lake-terminating glaciers are north-facing (Fig. 1c), with 385 (~66.61%) oriented towards north, northeast, or northwest.

Observations indicate that 583 proglacial lakes are connected to glaciers, with an average area of  $0.28 \pm 0.03$  km<sup>2</sup>. Although only 217 proglacial lakes exceed 0.1 km<sup>2</sup>, they account for 92% of the

total proglacial lake area (Fig. 3a). Most lakes (~64%) are situated at elevations between 4800 and 5500 m a.s.l. (Fig. 3b). Notably, the number of lake-terminating glaciers does not correspond directly to proglacial lakes. Our results revealed that there are three types of glacier–lake contact (Fig. 4): 564 glaciers host a single proglacial lake, 7 glaciers develop multiple proglacial lakes and 2 proglacial lakes interact and receive inflow from multiple glaciers.

# 4.2. Change of lake-terminating glaciers between 1990 and 2020

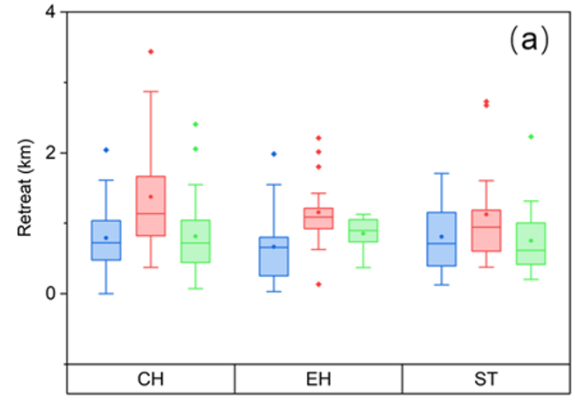
Between 1990 and 2020, the number of lake-terminating glaciers increased by 158, representing a 38% growth. This change resulted from two concurrent processes: the formation of new proglacial lakes (quantitative increase) and glacier–lake detachment events (quantitative decrease). Among the three identified glacier change types, Type 2 change glaciers (transition from supraglacial to proglacial lakes) are the most prevalent (Fig. 1b), totaling 331. These glaciers also exhibit the smallest mean area (2.4 km², Fig. 3d). In contrast, Type 3 change glaciers (proglacial lakes became detached from their parent glacier) have the largest mean area (7.7 km²). These glaciers area primarily face north-facing, including north, northeast and northwest orientation (Fig. 1c), and







Figure 4. Examples showing multiple glaciers contributing to a single proglacial lake, and one glacier connecting with multiple proglacial lakes.



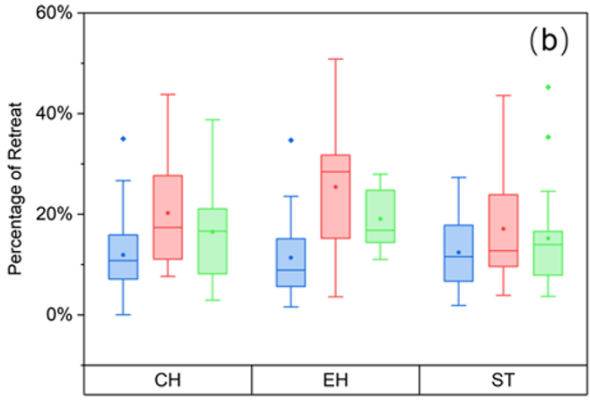


Figure 5. The boxplots for glacial terminus retreat (a) and percentage of retreat (b) illustrate the distribution of retreat distances and relative retreat percentages across different glacier types. The interquartile range (IQR) is represented by the box, the median by the central bar and the mean by a dot. Blue, red and green colors correspond to Type 1 change, Type 2 change and Type 3 change glacier, respectively. CH: Central Himalaya. EH: Eastern Himalaya. ST: Southeastern Tibet.

show similar elevation distributions, primarily clustered between 5000 and 6000 m a.s.l. (Fig. 3b). Over the study period, lake-terminating glaciers collectively lost  $161.2 \pm 18.1 \text{ km}^2$  in terminus area. The greatest decrease was observed in Type 1 change glaciers (73.8  $\pm$  13.1 km²), followed by Type 2 change glaciers (56.0  $\pm$  10.9 km²) and Type 3 change glaciers (31.4  $\pm$  6.0 km²).

We compared glacier dynamics—including length, surface elevation and flow velocity changes—across different glacier types within each subregion. To reduce uncertainties, glaciers smaller than  $2\,\mathrm{km}^2$  were excluded from the analysis. The Western Himalaya subregion was omitted due to insufficient sample size (n < 5) meeting the  $2\,\mathrm{km}^2$  threshold.

### 4.2.1 Glacier retreat

Across three subregions, Type 2 change glaciers exhibited greater median terminus retreat compared to Type 1 change and Type 3 change glaciers (Fig. 5). Statistically significant differences (Table S1 and S2) were observed in the Central and Eastern Himalaya. In the Central Himalaya, Type 2 change glaciers retreated 1.13 ± 0.24 km, significantly more than that Type 1 change  $(0.72 \pm 0.06 \text{ km}, p < 0.001)$  and Type 3 change  $(0.72 \pm 0.09 \text{ km},$ p = 0.003). Similarly, in the Eastern Himalaya, Type 2 change glaciers retreated  $1.09 \pm 0.06$  km, significantly exceeding the retreat of Type 1 change glaciers (0.66  $\pm$  0.08 km, p = 0.003). Regarding relative retreat (Fig. 5), significant differences were observed in the Central Himalaya between Type 1 change glaciers (10.8  $\pm$  0.9%) and both Type 2 change (17.4  $\pm$  3.0%, p = 0.019) and Type 3 change  $(16.6 \pm 1.6\%, p = 0.047)$  glaciers. In the Eastern Himalaya, Type 2 change glacier (28.5  $\pm$  2.8%, p < 0.001) and Type 3 change glaciers  $(16.8 \pm 2.0\%, p = 0.036)$  also exhibited significantly higher relative retreat than Type 1 change glaciers (8.9  $\pm$  1.6%).

#### 4.2.2 Glacier surface elevation change and ice flow velocities

Statistical analysis revealed no significant differences in glacier surface elevation changes among the three types of lake-terminating glaciers across the four subregions (Table S6). In the Eastern Himalaya, Type 2 change glaciers ( $-0.85 \pm 0.10$  m a<sup>-1</sup>) exhibited more pronounced thinning compared to Type 1 change glacier ( $-0.63 \pm 0.07$  m a<sup>-1</sup>) and Type 3 change glaciers ( $-0.77 \pm 0.07$  m a<sup>-1</sup>), as visually illustrated in Fig. 6.

Glacier velocity analyses revealed distinct elevation distribution patterns during the study period (Fig. 7). In the Central Himalaya, the median peak velocity of Type 1 change glaciers (5.32  $\pm$  1.02 m a<sup>-1</sup>, bin 0.1) occurs at a lower elevation than that of Type 2 change glacier (3.86  $\pm$  1.40 m a<sup>-1</sup>, 0.2) and Type 3 change glaciers (3.62  $\pm$  0.43 m a<sup>-1</sup>, bin 0.2). Similarly, in the Eastern Himalaya, Type 2 change glaciers (4.56  $\pm$  2.84 m a<sup>-1</sup>, bin 0.1) reach their median peak velocity at a lower elevation than Type 1 change (5.45  $\pm$  2.16 m a<sup>-1</sup>, bin 0.2) and Type 3 change glaciers (5.56  $\pm$  0.69 m a<sup>-1</sup>, bin 0.3). In Southeastern Tibet, Type 1 change glaciers (5.73  $\pm$  1.57 m a<sup>-1</sup>, bin 0.1) also exhibit median peak velocity at lower elevation compared to Type 2 change glacier (7.39  $\pm$  1.93 m a<sup>-1</sup>, bin 0.2) and Type 3 change glaciers (4.18  $\pm$  0.97 m a<sup>-1</sup>, bin 0.5).

During 1990–2018, all glacier types exhibited negative trends in median velocity anomalies (Fig. 8), except for Type 1 change glaciers in the Eastern Himalaya, which showed a marginal acceleration ( $0.06 \pm 0.01 \, \mathrm{m \, a^{-1}}$  decade<sup>-1</sup>, p = 0.59). Type 2 change glaciers displayed the most pronounced negative velocity anomaly trends across subregions, with statistical significance. In the Central Himalaya, this rate was  $-0.34 \pm 0.05 \, \mathrm{m \, a^{-1}}$  decade<sup>-1</sup> (p < 0.001), while in the Eastern Himalaya, it reached  $-0.45 \pm 0.11 \, \mathrm{m \, a^{-1}}$  decade<sup>-1</sup> (p < 0.001). In Southeastern Tibet, Type 2 change glaciers exhibited a rate of  $-0.38 \pm 0.08 \, \mathrm{m \, a^{-1}}$  decade<sup>-1</sup> (p < 0.001).

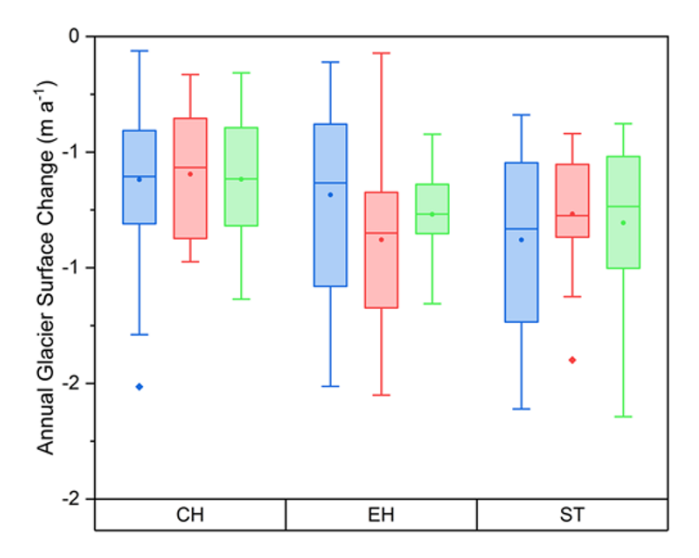


**Figure 6.** Boxplot illustrates the distribution of median surface elevation changes within glacier extents for different glacier types across each subregion. The interquartile range (IQR) is represented by the box, the median by the central bar and the mean by a dot. Blue, red and green colors correspond to Type 1 change, Type 2 change and Type 3 change glacier, respectively. CH: Central Himalaya. EH: Eastern Himalaya. ST: Southeastern Tibet.

To further examine the impact of changes in glacier–lake contact on glacier terminus dynamics, we selected glaciers larger than  $5~\rm km^2$ . This threshold ensured sufficient valid pixels for analysis despite glacier shrinking and the limited spatial resolution of the dataset (240 m). Velocity change trends were then tracked in the terminal 25% region of Type 1 change glaciers (n = 79, Table S7) and Type 3 change glaciers (n = 27, Table S8). Among Type 1 change glaciers, 56 exhibited deceleration trends, with 38 showing statistically significant trends, while 23 exhibited acceleration trends, of which 11 were statistically significant. In contrast, among Type 3 change glaciers, 23 showed deceleration and 4 exhibited acceleration trends, with 18 displaying statistically significant trends—all of which were associated with deceleration. Type 2 change glaciers were excluded from velocity trend analysis due to insufficient temporal resolution of lake formation data.

# 5. Discussion

# 5.1. Uncertainties in the lake-terminating glacier dataset and comparison with other lake datasets

The calculated error indicates that the total absolute area error in lake-terminating glaciers was approximately  $\pm$  13.1 km² in 1990 and  $\pm$  12.3 km² in 2020, with mean relative error was  $\pm$  12.5% and  $\pm$  13.8%, respectively. Individual glacier relative errors varied considerably (1–68%), and exhibited a strong power law relationship with glacier size ( $E_g=0.10988\times S^{-0.42384},\ R^2=0.88$ , Fig. 9a). Parallel analysis of proglacial lakes showed total absolute area errors of  $\pm$  0.57 km² and  $\pm$  0.73 km², with mean relative errors of  $\pm$  18.02% and  $\pm$  21.10% in 1990 and 2020, respectively. Relative errors for individual lakes ranged from 2% to 57% and similarly followed a significant power law dependency on lake area ( $E_l=0.05286\times A^{-0.45000}$ ,  $R^2=0.94$ , Fig. 9b). These analyses revealed an inverse relationship between feature size and measurement precision: both glacier and proglacial lake dimensions were significantly negative correlated with relative area errors

(p < 0.01), indicating smaller features were associated with greater uncertainty, consistent with the observed power law dependencies.

Among publicly available datasets covering the Himalava and Southeastern Tibet, the inventory compiled by Zhang and others, (2023) provides detailed classification of proglacial lakes with temporal coverage matching our study period. Therefore, we conducted a comparative analysis primarily against their dataset. According to their records, the study area contained 512 proglacial lakes (total area: 121.87 km<sup>2</sup>) in 1990 and 816 lakes (178.51 km<sup>2</sup>) in 2020. These figures exceed our inventory by 95 lakes (12.10 km<sup>2</sup>) and 233 lakes (15.65 km<sup>2</sup>) for the respective years. For laketerminating glaciers, we selected candidates from the RGI 6.0 dataset using the glacial lake inventory provided by Zhang and others, (2023) for comparison. Based on their dataset, the number of identified lake-terminating glaciers was 491 in 1990 and 758 in 2020, exceeding our corresponding figures by 72 and 181 glaciers, respectively. In 1990, 331 glaciers were consistently identified as lake-terminating in both datasets. Additionally, 88 glaciers were classified as lake-terminating only in our study, while 160 were identified exclusively Zhang and others, (2023). Similarly, in 2020, 485 glaciers were jointly recognized as lake-terminating. Meanwhile, 92 glaciers were identified as lake-terminating only in our study and 273 only in Zhang and others, (2023).

The observed discrepancies are likely attributed to the stringent criteria adopted for lake-terminating glacier identification (Section 3.2). Specifically, our identification strategy emphasizes three aspects: (1) the relative positioning of the glacier and its proglacial lake, requiring that the lake be located at the glacier terminus along the flow direction; (2) a comprehensive assessment of glacier–lake contact, based on the temporal evolution of the lake and glacier surface geomorphology; and (3) the exclusion of ambiguous cases to ensure the reliability of classification.

### 5.2. The changing glacier-lake interactions

Glacier-lake contact is a dynamic process, encompassing both the formation of proglacial lakes (Type 2 change glaciers) and the separation of the glacier from their lake (Type 3 change glaciers). In 2020, many Type 2 change glaciers were observed, accounting for nearly 60% of all lake-terminating glaciers. Notably, almost 70% of Type 2 change glaciers had an area smaller than 1 km<sup>2</sup>, with a median area of  $0.51 \pm 0.41$  km<sup>2</sup>. The sensitivity of small glaciers to climate change varies considerably. In some regions, while larger glaciers undergo rapid melting and retreating, small glaciers may remain relatively stable (Granshaw and Fountain, 2006; DeBeer and Sharp, 2009). Huss and Fischer (2016) reported in the Alps that small glaciers are particularly sensitive to climate change when situated on gentler slopes, covered by debris, or located at lower elevations. As proglacial lakes form on small glaciers, their impact on these glaciers cannot be ignored. This may lead to further differentiation in regional glacier changes.

The separation of proglacial lakes from glaciers is primarily driven by changes in glacier terminus slope and a decline in proglacial lake water level. However, only eight glaciers experienced separation from their proglacial lakes due to lake level decline (Figure S7), six of which were associated with documented GLOFs with clear historical flood records (Lützow and others, 2023; Shrestha and others, 2023). Slope analysis along the normalized flowlines of Type 1 change and Type 3 change glaciers shows that Type 3 change glaciers exhibit steeper terminal slopes than Type 1 change glaciers (Fig. 10). Such steepening indicates a

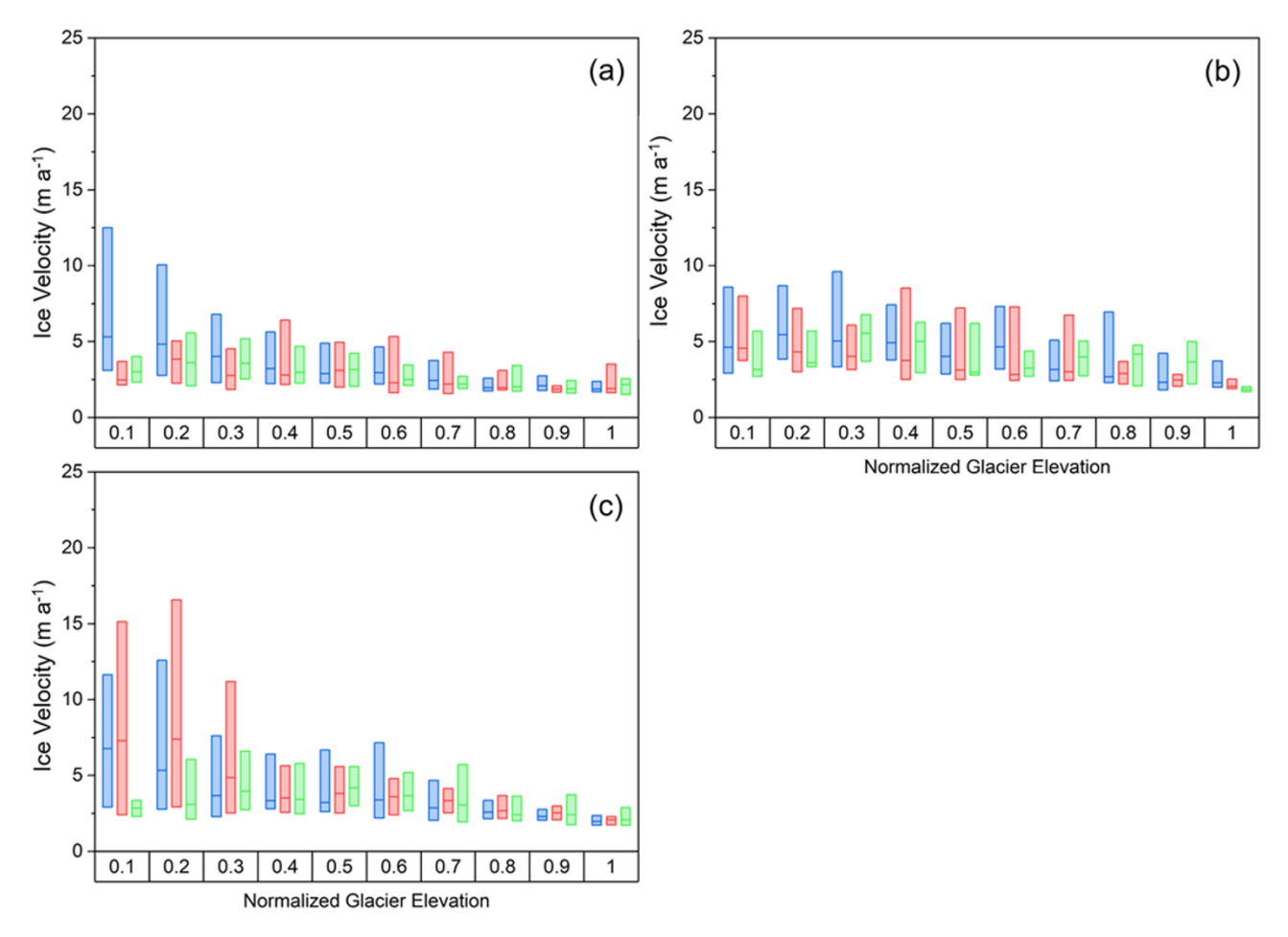


Figure 7. Median velocity across normalized glacier elevation between 1990 and 2018 in (a) Central Himalaya, (b) Eastern Himalaya and (c) Southeastern Tibet. The interquartile range (IQR) is represented by the box, the median by the central bar. Blue, red and green colors correspond to Type 1 change, Type 2 change and Type 3 change glacier, respectively.

contraction of the lake basin, which restricts further lake expansion towards the glaciers. Consequently, as the glacier retreats, the proglacial lake becomes detached from the glacier terminus.

# 5.3. Influence of glacier-lake contact change on glacier evolution

Although the differences in glacier surface elevation changes among glacier types within each subregion did not reach statistical significance, observational data reveal noteworthy variations. In the Eastern Himalaya, Type 2 change glaciers exhibit a more negative mean glacier surface elevation change rate  $(-0.85 \pm 0.10 \text{ m})$  $a^{-1}$ ) compared to Type 1 change glaciers ( $-0.63 \pm 0.07 \text{ m a}^{-1}$ ), with a visually apparent distinction (Fig. 6). Additionally, the terminus retreat distance of Type 2 change glaciers (1.09 ± 0.06 km) is greater than that of Type 1 change glaciers (0.66  $\pm$  0.08 km), with statistical significance (p = 0.003). This suggests a negative impact of proglacial lake expansion on glacier surface elevation change, a phenomenon also reported in the Alps (Carrivick and others, 2022) and Patagonia (Minowa and others, 2023). In the Central Himalaya, Type 2 change glaciers exhibit statistically significant retreat compared to Type 1 (p < 0.001) and Type 3 (p = 0.003) change glaciers and, yet their surface elevation changes show no substantial divergence. This discrepancy likely reflects a temporal misalignment between the phase of rapid glacier retreat and the observational period for surface elevation change.

Analysis revealed diverse patterns in the terminal velocity change of lake-terminating glaciers. While glacier motion in HMA is generally decelerating due to enhanced surface melting (Neckel and others, 2017; Dehecq and others, 2018), our results show that among Type 1 change glaciers (>5 km<sup>2</sup>), 49 exhibited significant terminal velocity trends, with 11 accelerating and 38 decelerating. It is commonly understood that when glacier termini approach flotation, basal stress decreases sharply, resulting in glacier acceleration (Benn and others, 2007b). Conversely, glaciers respond dynamically to the stress imbalance at the terminus through dynamic thinning, leading to a subsequent slowdown of flow (Nick and others, 2009; Pronk and others, 2021). However, this process appears to represent a relatively short-term and cyclical behavior, as also observed in the periodic flow variations of the Longbasaba Glacier (Liu and others, 2020). Such cyclicity typically induces glacier acceleration during phases of dynamic thinning, but deceleration emerges once thinning approaches completion. In addition, terminus deceleration may also be attributed to several factors, including enhanced lateral friction due to glacier narrowing (King and others, 2018), ice thickness decreases (Pronk and others, 2021), or insufficient lake depth (Minowa and others, 2023). As proglacial lakes detach from glaciers, lake influence diminishes, leading to a pronounced reduction in terminal velocities. Among

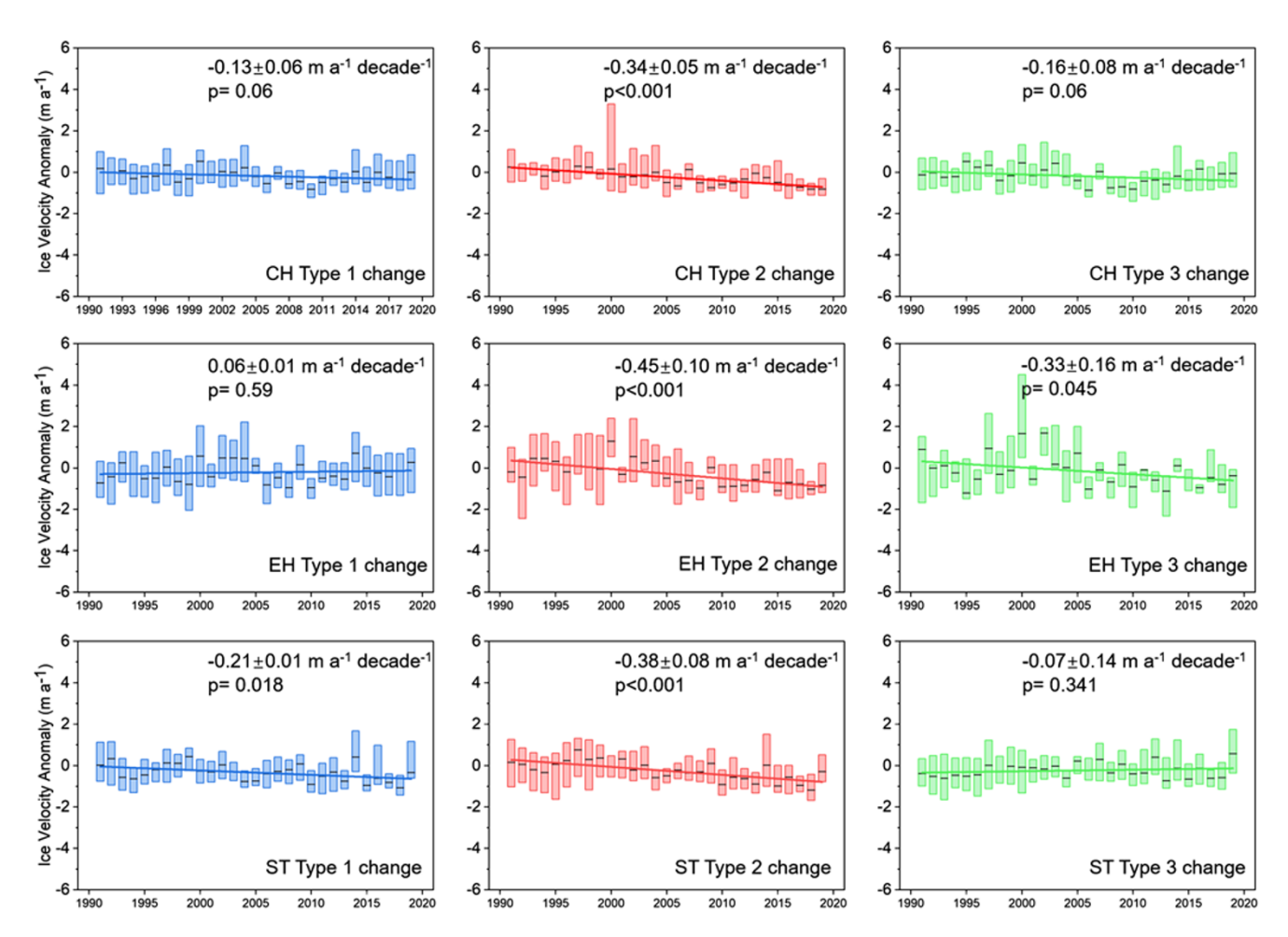


Figure 8. Annual glacier velocity anomalies for different glaciers (1990–2018). Black lines indicate the median anomaly, color bars represent the interquartile range and colored lines depict the linear trend. CH: Central Himalaya. EH: Eastern Himalaya. ST: Southeastern Tibet.

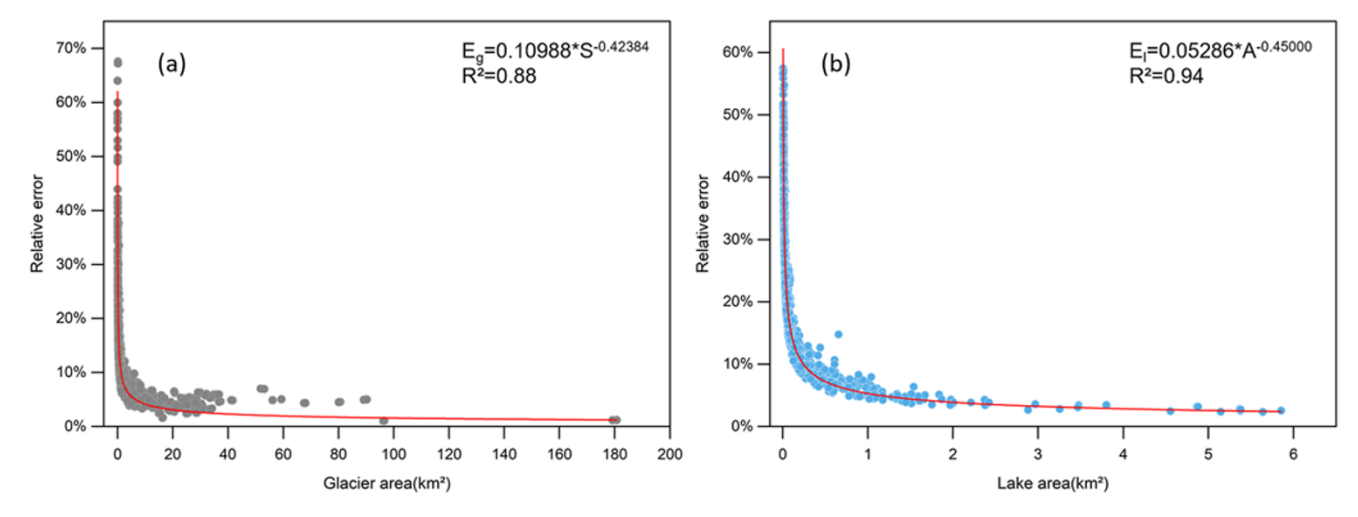
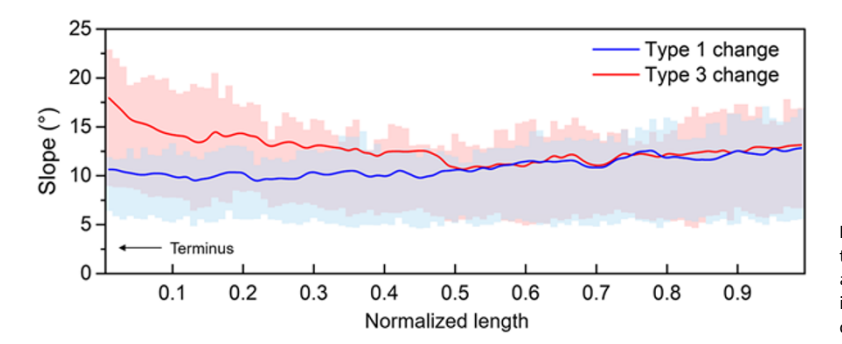


Figure 9. Relationships of relative area error against size of glacier (a) and glacial lakes (b).

Type 3 change glaciers (>5 km²), all 18 with significant velocity trends decelerated. Additionally, the migration of peak flow velocities to higher elevation bins (Fig. 7) of all Type 3 change glaciers. Overall, glacier velocity changes reflect complex, stage-dependent interactions between retreat dynamics and lake characteristics. These trends exhibit considerable individual variability, governed

by factors such as lake basin geometry, surrounding topography, glacier width, surface slope and ice thickness. And, variations in glacier-lake contact significantly influence glacier dynamics. To improve understanding of proglacial lake impacts on glacier dynamics, high-resolution, spatiotemporal analyses of glacier-lake co-evolution are required. Critical measurements include lake



**Figure 10.** Glacier slope along the normalized glacier center flow line at the ablation zone. The lines represent the mean values, while the shaded areas indicate the interquartile range. Type 1 change: Glaciers that keep in contact with proglacial lakes (n=146). Type 3 change: Glaciers become detached from proglacial lakes (n=173).

depth, basin morphology, water temperatures near the calving front and glacier thickness, which together will provide essential constraints on the processes driving the behavior of laketerminating glaciers.

**Data availability statement.** The data sets of the glacier and glacial lake for this study can be found and downloaded from https://doi.org/10.5281/zenodo.

### 6. Conclusions

We investigated the spatiotemporal distribution and dynamics of lake-terminating glaciers in the Himalaya and Southeastern Tibet from 1990 to 2020. Over the past three decades, the number of lake-terminating glaciers increased by 37.7% (from 419 to 577), whereas their total area was decreased by 161.2 ± 18.1 km<sup>2</sup> due to pronounced calving retreat. During this period, 173 glaciers detached from their proglacial lakes, while 331 developed new proglacial lakes. Terminus steepening was the primary driver of glacier-lake separation, with reductions or loss of lake water levels, though rare (n = 8), also contributing. Based on glacier-lake contact changes, glaciers were classified as Type 1 change (persistent contact, n = 246), Type 2 change (new lake formation, n = 331) and Type 3 change (detachment, n = 173). Type 1 change glaciers experienced the largest area loss (73.8  $\pm$  13.1 km<sup>2</sup>), while Type 2 change glaciers were most numerous. Glacier-lake contact variations significantly modulate glacier dynamics. Among Type 1 change glaciers (>5 km<sup>2</sup>), 49 exhibited significant velocity changes, with 22.4% (n = 11) accelerating and 77.6% (n = 38) decelerating, whereas all 18 Type 3 change glaciers (>5 km<sup>2</sup>) with significant trends decelerated. These findings highlight the crucial role of glacier-lake interactions in modulating glacier behavior. However, the lack of in situ observational data limits our understanding of glacier-lake interactions and their variations in this region, particularly regarding lake basin morphology, water depth changes and high temporal resolution monitoring of lake expansion. This is essential for accurately assessing glacier dynamics, developing glacier dynamics and hydro-mathematical models, comprehending glacial chain-related hazards and managing the risks associated with GLOFs.

**Supplementary material.** The supplementary material for this article can be found at https://doi.org/10.1017/jog.2025.10088.

**Acknowledgements.** This work was funded by the National Key R&D Program of China (Grant Nos. 2024YFC3013400 and 2023YFE0102800), National Science Foundation of China (Grant Nos. 42361144874 and 42401101), Science and Technology Plan Projects of Tibet Autonomous Region (XZ202301YD0002C-03) and Institute of Mountain Hazards and Environment (Grant No. IMHE-CXTD-02). We would like to express our thanks to the editors and two anonymous reviewers for their constructive comments and suggestions which ultimately led to an improved manuscript.

#### References

Agarwal V and 6 others (2023) Long-term analysis of glaciers and glacier lakes in the Central and Eastern Himalaya. Science of the Total Environment 898, 165598. doi: 10.1016/j.scitotenv.2023.165598.

**Ageta Y and Higuchi K** (1984) Estimation of mass balance components of a summer-accumulation type Glacier in the Nepal Himalaya. *Geografiska Annaler: Series A, Physical Geography* **66**(3), 249–255. doi: 10.1080/04353676.1984.11880113.

Benn DI, Warren CR and Mottram RH (2007a) Calving processes and the dynamics of calving glaciers. *Earth-Science Reviews* **82**(3-4), 143–179. doi: 10.1016/j.earscirev.2007.02.002.

Benn DI, Hulton NRJ and Mottram RH (2007b) 'Calving laws', 'sliding laws' and the stability of tidewater glaciers. *Annals of Glaciology* **46**, 123–130. doi: 10.3189/172756407782871161.

Bolch T, Menounos B and Wheate R (2010) Landsat-based inventory of glaciers in western Canada, 1985–2005. *Remote Sensing of Environment* 114(1), 127–137. doi: 10.1016/j.rse.2009.08.015.

Bookhagen B and Burbank DW (2010) Toward a complete Himalayan hydrological budget: Spatiotemporal distribution of snowmelt and rainfall and their impact on river discharge. *Journal of Geophysical Research: Earth Surface* 115(F3), F03019. doi: 10.1029/2009]F001426.

Brun F and 6 others (2019) Heterogeneous influence of glacier morphology on the mass balance variability in high mountain Asia. *Journal of Geophysical Research-Earth Surface* **124**(6), 1331–1345. doi: 10.1029/2018jf004838.

Brun F, Berthier E, Wagnon P, Kaab A and Treichler D (2017) A spatially resolved estimate of high mountain Asia glacier mass balances, 2000-2016. *Nature Geoscience* 10(9), 668–673. doi: 10.1038/NGEO2999.

Carrivick JL and 7 others (2022) Coincident evolution of glaciers and icemarginal proglacial lakes across the Southern Alps, New Zealand: Past, present and future. *Global and Planetary Change* 211, 103792. doi: 10.1016/j.gloplacha.2022.103792.

Carrivick JL and Tweed FS (2013) Proglacial lakes: Character, behaviour and geological importance. *Quaternary Science Reviews* 78, 7834–7852. doi: 10. 1016/j.quascirev.2013.07.028.

Chen F and 6 others (2021) Annual 30 m dataset for glacial lakes in High Mountain Asia from 2008 to 2017. Earth System Science Data 13(2), 741–766. doi: 10.5194/essd-13-741-2021.

**DeBeer CM and Sharp MJ** (2009) Topographic influences on recent changes of very small glaciers in the Monashee Mountains, British Columbia, Canada. *Journal of Glaciology* **55**(192), 691–700. doi: 10.3189/002214309789470851.

Dehecq A and 9 others (2018) Twenty-first century glacier slowdown driven by mass loss in High Mountain Asia. *Nature Geoscience* 12(1), 22–27. doi: 10.1038/s41561-018-0271-9.

**Dou X** and **5 others** (2023) The response of glaciers and glacial lakes to climate change in the Southeastern Tibetan Plateau over the past three decades. *Land Degradation & Development* **34**(18), 5675–5696. doi: 10.1002/ldr.4870.

**Foga S** and **9 others** (2017) Cloud detection algorithm comparison and validation for operational Landsat data products. *Remote Sensing of Environment* **194**, 379–390. doi: 10.1016/j.rse.2017.03.026.

- Granshaw FD and Fountain A (2006) Glacier change (1958–1998) in the North Cascades National Park Complex, Washington, USA. *Journal of Glaciology* **52**(177), 251–256. doi: 10.3189/172756506781828782.
- Hanshaw MN and Bookhagen B (2014) Glacial areas, lake areas, and snow lines from 1975 to 2012: Status of the Cordillera Vilcanota, including the Quelccaya Ice Cap, northern central Andes, Peru. *The Cryosphere* 8(2), 359–376. doi: 10.5194/tc-8-359-2014.
- **Hugonnet R** and **10 others** (2021) Accelerated global glacier mass loss in the early twenty-first century. *Nature* **592**(7856), 726–731. doi: 10.1038/s41586-021-03436-z.
- **Huss M and Fischer M** (2016) Sensitivity of very small glaciers in the Swiss Alps to future climate change. *Frontiers in Earth Science* 4. doi: 10.3389/feart.2016. 00034.
- Kienholz C, Rich JL, Arendt AA and Hock R (2014) A new method for deriving glacier centerlines applied to glaciers in Alaska and northwest Canada. The Cryosphere 8(2), 503–519. doi: 10.5194/tc-8-503-2014.
- King O, Dehecq A, Quincey D and Carrivick J (2018) Contrasting geometric and dynamic evolution of lake and land-terminating glaciers in the central Himalaya. Global and Planetary Change 167, 46–60. doi: 10.1016/j.gloplacha. 2018.05.006.
- King O, Quincey DJ, Carrivick JL and Rowan AV (2017) Spatial variability in mass loss of glaciers in the Everest region, central Himalayas, between 2000 and 2015. *The Cryosphere* 11(1), 407–426.
- Kumar P, Sharma S and Bahuguna I (2024) Spatio-temporal change analysis of glacial lakes in Himachal Himalayas using geospatial technology. International Journal of Advanced Technology and Engineering Exploration 11(117), 1111.
- Li D, Shangguan D and Anjum MN (2020) Glacial lake inventory derived from Landsat 8 oli in 2016–2018 in China–Pakistan Economic Corridor. *ISPRS International Journal of Geo-Information* **9**(5). doi: 10.3390/ijgj9050294.
- Li J and Sheng Y (2012) An automated scheme for glacial lake dynamics mapping using Landsat imagery and digital elevation models: A case study in the Himalayas. *International Journal of Remote Sensing* 33(16), 5194–5213. doi: 10.1080/01431161.2012.657370.
- **Liu Q** and **6 others** (2020) Interannual flow dynamics driven by frontal retreat of a lake-terminating glacier in the Chinese Central Himalaya. *Earth and Planetary Science Letters* **546**, 116450. doi: 10.1016/j.epsl.2020.116450.
- **Luo W, Zhang G, Chen W and Xu F** (2020) Response of glacial lakes to glacier and climate changes in the western Nyainqentanglha range. *Science of the Total Environment* **735**, 139607. doi: 10.1016/j.scitotenv.2020.139607.
- Lützow N, Veh G and Korup O (2023) A global database of historic glacier lake outburst floods. Earth System Science Data 15(7), 2983–3000. doi: 10.5194/ essd-15-2983-2023.
- Maussion F and 14 others (2019) The Open Global Glacier Model (OGGM) v1.1. Geoscientific Model Development 12, 909–931. doi: 10.5194/gmd-12-909-2019.
- Minowa M, Schaefer M and Skvarca P (2023) Effects of topography on dynamics and mass loss of lake-terminating glaciers in southern Patagonia. *Journal of Glaciology* **69**(278), 1580–1597. doi: 10.1017/jog.2023.42.

- Neckel N, Loibl D and Rankl M (2017) Recent slowdown and thinning of debris-covered glaciers in South-Eastern Tibet. Earth and Planetary Science Letters 464, 95–102. doi: 10.1016/j.epsl.2017.02.008.
- Nick FM, Vieli A, Howat IM and Joughin I (2009) Large-scale changes in Greenland outlet glacier dynamics triggered at the terminus. *Nature Geoscience* 2(2), 110–114. doi: 10.1038/ngeo394.
- Pronk JB, Bolch T, King O, Wouters B and Benn DI (2021) Contrasting surface velocities between lake- and land-terminating glaciers in the Himalayan region. *The Cryosphere* 15(12), 5577–5599. doi: 10.5194/tc-15-5577-2021.
- **Quincey DJ** and **6 others** (2007) Early recognition of glacial lake hazards in the Himalaya using remote sensing datasets. *Global and Planetary Change* **56**(1-2), 137–152. doi: 10.1016/j.gloplacha.2006.07.013.
- RGI Consortium (2017) Randolph Glacier Inventory A Dataset of Global Glacier Outlines, Version 6. Boulder, Colorado USA. NSIDC: National Snow and Ice Data Center.
- Salerno F and 6 others (2012) Glacial lake distribution in the Mount Everest Region: Uncertainty of measurement and conditions of formation. Global and Planetary Change 92–9330–39. doi: 10.1016/j.gloplacha.2012.04.001.
- Scoffield AC and 5 others (2024) Sub-regional variability in the influence of ice-contact lakes on Himalayan glaciers. *Journal of Glaciology* 70(e15), doi: 10.1017/jog.2024.9.
- Shrestha F and 9 others (2023) A comprehensive and version-controlled database of glacial lake outburst floods in High Mountain Asia. Earth System Science Data 15(9), 3941–3961. doi: 10.5194/essd-15-3941-2023.
- Sugiyama S and 7 others (2011) Ice speed of a calving glacier modulated by small fluctuations in basal water pressure. *Nature Geoscience* 4(9), 597–600. doi: 10.1038/ngeo1218.
- Sutherland JL and 5 others (2020) Proglacial lakes control glacier geometry and behavior during recession. Geophysical Research Letters 47(19), doi: 10. 1029/2020gl088865.
- Truffer M and Motyka RJ (2016) Where glaciers meet water: Subaqueous melt and its relevance to glaciers in various settings. Reviews of Geophysics 54(1), 220–239. doi: 10.1002/2015rg000494.
- **Tsutaki S** and **6 others** (2019) Contrasting thinning patterns between lake- and land-terminating glaciers in the Bhutanese Himalaya. *The Cryosphere* **13**(10), 2733–2750. doi: 10.5194/tc-13-2733-2019.
- Wang X and 9 others (2020) Glacial lake inventory of high-mountain Asia in 1990 and 2018 derived from Landsat images. Earth System Science Data 12(3), 2169–2182. doi: 10.5194/essd-12-2169-2020.
- Warren CR and Kirkbride MP (2003) Calving speed and climatic sensitivity of New Zealand lake-calving glaciers. Annals of Glaciology 36, 173–178. doi: 10.3189/172756403781816446.
- Zhang G (2017) Automated water classification in the Tibetan plateau using Chinese gf-1 wfv data. *Photogrammetric Engineering & Remote Sensing* 83(7), 509–519. (and 5 others) doi: 10.14358/pers.83.7.509.
- Zhang G and 5 others (2023) Underestimated mass loss from lake-terminating glaciers in the greater Himalaya. *Nature Geoscience* 16(4), 333–338. doi: 10. 1038/s41561-023-01150-1.
- Zheng G and 11 others (2021) Increasing risk of glacial lake outburst floods from future Third Pole deglaciation. *Nature Climate Change* 11(5), 411–417. doi: 10.1038/s41558-021-01028-3.